Comparison of the approaches to the solution of the outer Magneto-Static-Problem in free-boundary MHD solvers

N. Isernia[1], G. Rubinacci[1], N. Schwarz[2], R. Sparago[1,4], F. Vannini[2], S. Ventre[3], M. Hoelzl[2], F. J. Artola[4], F. Villone[1]

[1] *CREATE, Università degli Studi di Napoli Federico II, DIETI, 80125 Napoli, Italy*

[2] *Max Planck Institute for Plasma Physics, Boltzmannstr. 2, 85748 Garching, Germany*

[3] *CREATE, Università di Cassino e del Lazio Meridionale, DIEI, 03043 Cassino, Italy*

[4] *ITER Organization, Route de Vinon sur Verdon, 13067 St Paul Lez Durance Cedex, France*

The solution of free-boundary MHD problems, both static and dynamic, via Finite Element Methods requires the correct set up of the electro-magnetic boundary conditions at the boundary of the computational domain [1]. A convenient formulation of the problem reduces this general task to the problem of determining the magnetic field tangent to the boundary as a function of the magnetic vector potential tangent to the boundary itself, plus all the external currents. In the framework of extending the free-boundary capabilities of the JOREK code [2, 3], via its coupling with CARIDDI [4], we compare here three different implementations of the ideal Dirichlet-to-Neumann map in absence of external currents, *i.e.* three possible ways of computing the relation $A_{tan,pl} \rightarrow B_{tan,pl}$. The first two implementations are based on the virtual casing principle: an equivalent current to the plasma is defined at the boundary of the JOREK domain which describes the magnetic field outside. In implementation (A) the JOREK boundary is discretized via 3D hexahedral elements and the equivalent current to the plasma is represented via standard CARIDDI edge basis functions [6]. In solution (B) the surface equivalent current to the plasma, expressed in term of flux function, is decomposed in toroidal harmonics, as for JOREK primary variables, and the JOREK boundary is approximated via standard Lagrange 1D linear elements. Finally, the last solution (C) is based on a direct Boundary Element approach, which exploits the Fourier decomposition of JOREK variables along the toroidal angle. In implementation (C) potentials and fields are described directly within the JOREK finite element space. The accuracy of the three approaches is compared first against an assigned current distribution for which we have analytical solution. Finally, we compare the MHD evolution of a tearing mode for a circular high aspect ratio test-case. The different maps discussed provide coherent results, we sketch the pros and cons of the different strategies in the final section.

Mathematical Models

In this contribution, we compute the Dirichlet-to-Neumann map $A_{tan,pl} \to B_{tan,pl}$ only in the reduced MHD approximation, *i.e.* $\mathbf{A} = \psi\nabla\varphi$. In this case, the information about the magnetic vector potential is equivalent to the information about the stream function ψ, moreover the boundary condition required by the MHD code is precisely $(1/r)\partial\psi/\partial n$, *i.e.* a contribution to the poloidal magnetic field. The mathematical details behind implementation (A) were presented in [2, 5]. In the proposed approach (B) the only difference deals with the representation of plasma equivalent currents: here we use a Fourier decomposition along the toroidal angle similar to the one used for JOREK variables. We represent the equivalent current as $\mathbf{k_{eq}}(\mathbf{x}) = \nabla I \times \mathbf{n}$ where $I = \sum_{n=-\infty}^{\infty} \bar{I}_n(s)\exp(jn\varphi)$, where s is a poloidal coordinate along the boundary of the JOREK domain. The Fourier coefficients $\{\bar{I}_0(s), \bar{I}_1(s), \cdots\}$ are then discretized via standard 1D Lagrange elements. In approach (C) we solve directly the standard boundary integral equation[8]:

$$(1/2)\,\mathbf{A} = -\int_{\partial V_{in}} \left[G\left(\mathbf{B}' \times \hat{\mathbf{n}}'\right)\right] \mathrm{d}S' - \int_{\partial V_{in}} \left[\left(\mathbf{A}' \times \hat{\mathbf{n}}'\right) \times \nabla' G - \left(\mathbf{A}' \cdot \hat{\mathbf{n}}'\right)\nabla' G\right] \mathrm{d}S', \qquad (1)$$

where $G = 1/4\pi|\mathbf{x} - \mathbf{x}'|$. This is solved, via a Galerkin method, in the hypothesis of toroidal geometry (the JOREK boundary is axially symmetric) and in the reduced MHD ansatz, *i.e.* $\mathbf{A} = \psi\nabla\varphi$ and $\mathbf{B} = F_0\nabla\varphi + \nabla\psi \times \nabla\varphi$, where F_0 is assumed homogeneous. This means that we neglect any term in A_r, A_z or B_φ that would naturally appear in Equation (1). Both the scalar fields and the Green function G are expanded in a Fourier series along φ. The singularity of the Fourier coefficients of G is extracted as indicated in [7]. This is the same for all toroidal harmonics, allowing to tackle the problem of the integration of the singularity once for all the harmonics included in the MHD simulation.

Assessment of the response matrices

The test case examined in this manuscript is a simple circular high-aspect-ratio tokamak, where the major radius of the computational domain is $R = 10\,m$ and the minor radius is $b = 1\,m$. Before using the Dirichlet to Neumann maps discussed above into actual MHD simulations, we first verify the robustness of our computation via an analytical test case, also in order to assess the integration precision to use. The analytical test case under exam uses as source of magnetic field a toroidal wire placed at the centre of the MHD computational domain and titled of 3 deg about the x-axis. The reference magnetic field is found by a semi-analytic approach. We compute the poloidal flux ψ analytically at two surfaces shifted of $\pm\Delta$ respect to the surface where we want to compute the magnetic field. The normal derivative of the poloidal flux is

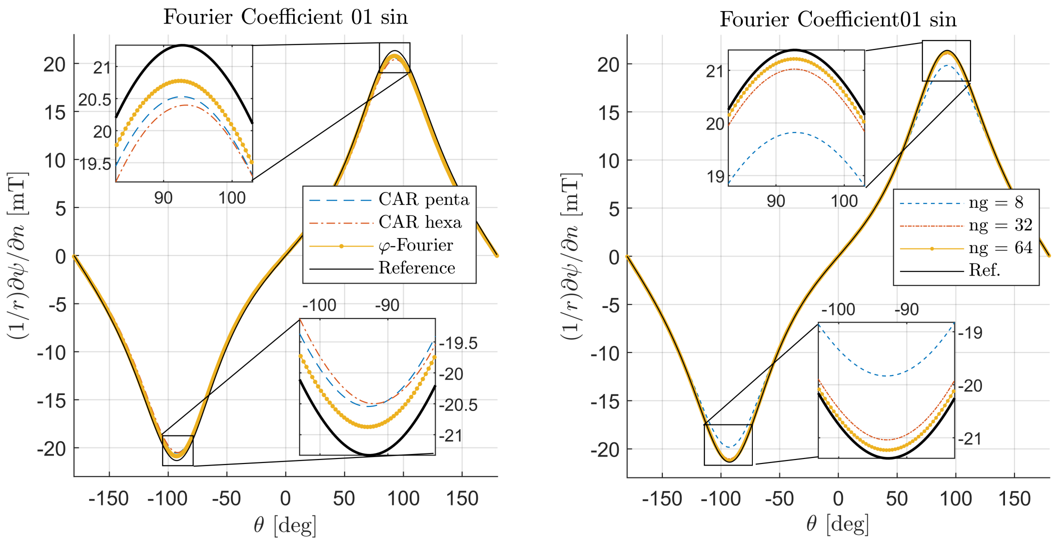

Figure 1: Tilted wire analytic test: poloidal magnetic field tangent to the boundary: (a) Virtual Casing principle with CARIDDI or 2D representation of the equivalent current; (b) Direct BEM for different integration precision.

then computed numerically. Decreasing progressively Δ up to 0.01 mm, we find that the magnetic field we use as reference is precise for our purposes. Notice that in case of the equivalent current methods (A) and (B) we compute the magnetic field at $1\,mm$ outside the boundary of the computational domain, while in the *direct* boundary element formulation (C) we compute the magnetic field precisely at the MHD domain boundary. The results of this assessment are reported in Figure 1. The left panel demonstrates that approach (B) is indeed coherent with the already assessed implementation (A). In the right panel, for method (C), we assess the number of integration points to use within a JOREK boundary element to reach sufficient precision.

No-wall tearing mode test case

In this Section we use the vacuum response matrix $A_{tan,pl} \to B_{tan,pl}$ to compute the evolution of an unstable tearing mode occurring in the circular high aspect ratio tokamak. The $q = 2$ surface is located quite close to the plasma boundary, hence very close to the boundary of the MHD computational domain. The external structures are set to high resistance, so that the interaction with eddy currents does not play a role in this exercise. The evolution of the magnetic energy for the $n = 1$ and $n = 2$ toroidal harmonics is reported in Figure 2, and the respective growth rates, as estimated via exponential fit, are reported in Table 1.

Conclusions

The immediate advantage of approaches (B) and (C) is that they allow not to discretize the MHD computational boundary along the toroidal angle, consistently with the representation of potentials and fields used in JOREK and many other MHD codes. This allows to save numerical

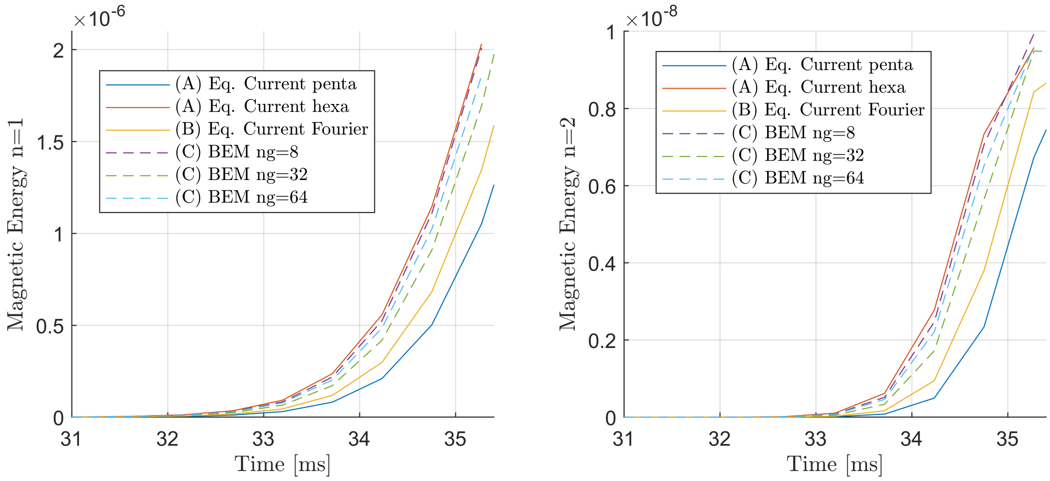

Figure 2: Evolution of the magnetic energies computed with the vacuum response matrices discussed in previous Sections.

	(A) penta	(A) hexa	(B) (fourier)	(C) ng=8	(C) ng=32	(C) ng=64
$n=1$	1.93kHz	1.93kHz	1.93kHz	1.96kHz	1.94kHz	1.93kHz
$n=2$	3.87kHz	3.87kHz	3.87kHz	3.92kHz	3.88kHz	3.87kHz

Table 1: Growth rate of the tearing mode instability as computed via the different maps. Exponential in the interval $[21.5, 33.5]$ ms.

resources in the actual computation of these vacuum-response matrices, especially if few harmonics are included in the MHD simulation. For scheme (A) and (B) the mathematical structure of the interaction with surrounding conductors can be implemented via the mutual inductance between equivalent plasma currents and external currents [6]. In scheme (C) Equation (1) can be used as a direct formula, anyway further discussion is necessary to get to a consistent interaction scheme. One difficulty in the implementation of scheme (C) regards the construction of the regular part of the Fourier coefficients of the Green function, which depend on the *source* and *field* point via the parameter $k^2 = 4RR'/[(R+R')^2 + (Z-Z')^2]$. Here we evaluated numerically and stored these functions only for the $n = 1$ and $n = 2$ harmonics, in a finite subset of points k^2 in the $[0, 1]$ interval. The procedure has to be assessed also for higher order harmonics.

Acknowledgements

This work has been carried out within the framework of the EUROfusion Consortium, funded by the European Union via the Euratom Research and Training Programme (Grant Agreement No 101052200 — EUROfusion). Views and opinions expressed are however those of the author(s) only and do not necessarily reflect those of the European Union or the European Commission. Neither the European Union nor the European Commission can be held responsible for them.

References

[1] B. Faugeras and H. Heumann, Journal of Computational Physics **343**, 201-216 (2017)
[2] M. Hoelzl et al., Journal of Physics: Conference Series **401**, 012010 (2012)
[3] M. Hoelzl et al., Nuclear Fusion **61**, 065001 (2021)
[4] R. Albanese and G. Rubinacci, IEE Proceedings A Physical Science, Meas. and Instr. **137**, 16-22 (1988)
[5] N. Isernia et al., Europhysics Conference Abstracts, **46A**, P1a.107 (48^{th} EPS Conf. on Plasma Physics, 2022)
[6] N. Isernia, N. Schwarz et al., submitted to Physics of Plasmas (2023)
[7] V. D. Pustovitov, Physics of Plasmas **15**, 072501 (2008)
[8] J. A. Stratton, Electromagnetic Theory (Mc-Graw Hill Book Company, 1941)